Multilevel Vibrational−Vibrational (V−V) Energy Transfer from CO(v) to O_2 and CO_2

Baoshan Wang and Yueshu Gu

School of Chemistry, Shandong University, Jinan, Shandong 250100, China

Fanao Kong*

The Institute of Chemistry, Chinese Academy of Sciences, Beijing 100080, China

Received: March 4, 1998; In Final Form: June 10, 1998

The vibrational−vibrational (V−V) energy transfer from excited CO($v \leq 10$) to O_2 and CO_2 molecules was studied by laser-induced chemiluminscence/time-resolved Fourier transform infrared emission spectroscopy. The vibrationally excited CO molecules were produced by 193 nm photolysis of a mixture of $CHBr_3$ and O_2. The temporal populations of the 10 vibrational states of CO were obtained from the time-resolved IR emission spectra. The rate equations were solved by a differential method we have suggested. Nine vibrational quenching rate constants k_v ($v = 1-9$) of O_2 were found to be 1.1 ± 0.1, 1.9 ± 0.1, 2.0 ± 0.2, 2.3 ± 0.3, 2.5 ± 0.3, 3.0 ± 0.3, 4.0 ± 0.5, 4.8 ± 0.5, and 8.0 ± 0.8 ($\times 10^{-14}$ cm^3 molecule^{-1} s^{-1}). And the k_v ($v = 1-8$) quenched by CO_2 were 5.7 ± 0.1, 5.9 ± 0.1, 5.3 ± 0.2, 3.4 ± 0.3, 2.4 ± 0.3, 2.2 ± 0.2, 2.0 ± 0.2, and 1.8 ± 0.2 ($\times 10^{-14}$ cm^3 molecule^{-1} s^{-1}), respectively. The trend of the (k_v) with v for CO/O_2 system was explained by a V−V energy transfer mechanism of single channel. For the CO/CO_2 system, a multichannel model, transferring the energy to the ν_1, ν_3, and several overtone vibrational modes of CO_2 molecule, was suggested. A modified SSH theoretical calculation fits well to the experimental data.

I. Introduction

The vibrational relaxation of gas molecules has been an active research field in the last few decades. The experimental techniques as well as the data analysis for vibrational relaxation and exchange have been reviewed in several articles.[1−4] The energy transfer from highly vibrational states of CO(v) to O_2 or to CO_2 molecules are of importance in high-temperature processes such as combustion. The previous investigations on the CO(v)/O_2 system were carried out only for the vibrational relaxation from $v = 1$ to 0. Bauer and Roesler[5] obtained a relaxation rate constant of $k_{1-0} = 1.5 \times 10^{-15}$ cm^3 molecule^{-1} s^{-1}. Using flash photoexcitation technique, Donovan and Husian[6] obtained the quenching rate of 1.0×10^{-14} cm^3 molecule^{-1} s^{-1}. To characterize temperature dependence, Miller and Millikan[7] studied the excited CO molecules by infrared radiation and obtained a quenching rate of 7.8×10^{-17} cm^3 molecule^{-1} s^{-1} at 300 K. In 1973, Green and Hancock[8] measured k_{1-0} to be 1.5×10^{-16} cm^3 molecule^{-1} s^{-1} by laser-induced fluorescence. As indicated above, there is a large discrepancy of 2 orders of magnitude between the measured rate constants.

In the previous studies, most of the experimental studies on the V−V energy transfer deal with the quenching from $v = 1$ to 0. The relaxation of highly vibrational states was scarcely studied. Only a few such reports appear in the literature. Two of these reports refer to the energy transfer from CO(v) to CO_2 system. Smith et al.[9] measured the vibrational exchange rate constants of CO(v) with CO_2 and obtained 10 rate constants for $v = 4-13$. In 1979, Murphy et al.[10] used a pulsed electron beam to initiate a reaction of CO_2/Ar mixture, and the emission from the excited product CO($v = 1-19$) was monitored by a time-resolved Fourier transform infrared (TR FTIR) spectrometer. Solving the rate equations, the vibrational relaxation rate constants of CO($v \rightarrow v-1$) to CO_2 for vibrational levels $v = 1-16$ were obtained.

In the past few years, the stimulated emission pumping (SEP) method has been employed to produce highly vibrationally excited states. Many papers report energy transfer from highly excited molecules.[4] However, the molecules should have an absorption in the visible or near UV region, such as I_2,[11−13] NO,[14−19] NO_2,[20−22] or O_2[23−28] molecules. So far it is difficult to stimulate CO molecules, which only absorb VUV light.

As first shown in Murphy's experiment, TR FTIR spectroscopy demonstrates many advantages in the study of vibrational energy transfer. The IR emission spectra simultaneously record various vibrational transitions and their temporal changes. It removes the fluctuations in experimental conditions which may be experienced in other sequential measurement techniques. But the electron beam excitation is not selective in Murphy's experiment. The vibrational excitation of CO_2 could also be caused by electron bombardment. Finally, the fluctuation of the electron beam current was difficult to get rid of.

In this paper, we report our study of the V−V energy transfer from the high vibrationally excited CO($v = 1-9$) to O_2 and to CO_2. The detection was made by TR FTIR spectroscopy. The excitation was initiated by a pulsed ultraviolet laser beam. This new technique is especially suitable for studying the collisional energy transfer between gas molecules, since the excitation laser can selectively generate highly vibrationally excited molecules, avoiding excitation of the collision partners.[29−31]

II. Experimental Section

The apparatus used was UV laser photolysis/time-resolved Fourier transform infrared spectrometer system which was described in details previously.[32] The system consists of three parts: an UV laser (Lambda Physik-305i), a reaction chamber, and a TR FTIR spectrometer (Nicolet 800). The UV light was used to initiate the photochemical reaction of $CHBr_3 + O_2$, producing vibrationally excited CO(v) molecule. The laser

10.1021/jp9813793 CCC: $15.00
Published on Web 10/10/1998

beam of 100 mJ per pulse at 193 nm was reduced to a size of 1×1 cm^2. The flowing pure O_2 gas or mixed gas of CO_2 and O_2 carried $CHBr_3$ vapor (Baker reagent, not further purified) into the vacuum chamber. The flow rate was adjusted by a flowmeter. At $T = 300$ K, the partial pressure of $CHBr_3$ was estimated to be 5 Pa. The pressure of O_2 was 200 Pa. In the system of CO/CO_2, the partial pressures of O_2 and CO_2 were 10 Pa and 120 Pa, respectively. The pressure in the chamber was monitored by a MKS manometer. In the chamber, a pair of parallel multilayer mirrors were used to reflect the laser beam 10 times. The laser photolysis zone is about $10 \times 5 \times 5$ cm^3. The IR emission was collected by a pair of gold-coated White-cell mirrors (nearly confocal), and collimated to the FTIR spectrometer, operating with a rapid scan mode. The spectral resolution was set at 16 cm^{-1}. To improve the signal-to-noise ratio, the sampling data were coadded for 20 times in the interferogram, and then were Fourier transformed.

A sequential time-resolved infrared emission spectra with an uncertainty of 5 μs were recorded. The background radiation of a blank experiment was subtracted. The instrumental spectral response and the absorption of H_2O and CO_2 were also corrected.

III. Method of Solving the Rate Equations

Considering the vibrational relaxation and the radiation processes

$$\mathrm{CO}(v{+}1) + \mathrm{M} \xrightarrow{k_{v+1}} \mathrm{CO}(v) + \mathrm{M}^* \quad (1)$$

$$\mathrm{CO}(v{+}1) \xrightarrow{A_{v+1}} \mathrm{CO}(v) + h\nu \quad (2)$$

$$\mathrm{CO}(v) + \mathrm{M} \xrightarrow{k_v} \mathrm{CO}(v{-}1) + \mathrm{M}^* \quad (3)$$

$$\mathrm{CO}(v) \xrightarrow{A_v} \mathrm{CO}(v{-}1) + h\nu \quad (4)$$

The related rate equation is

$$\frac{\mathrm{d}n_v}{\mathrm{d}t} = (k_{v+1}[\mathrm{M}] + A_{v+1})n_{v+1} - (k_v[\mathrm{M}] + A_v)n_v \qquad v = 1, 2, ..., \mathrm{N} \quad (5)$$

where n_v is the population of the vth vibrational level, k_v is the deactivation rate constant due to the quenching of M species, [M] is the number density of O_2 or CO_2, A_v is the Einstein coefficient, and N represents the highest vibrational level considered.

For a gaseous pressure of 200 Pa, the average free path of a gas molecule is about 30μm. The molecule will collide for $Z = 2 \times 10^4$ times in 1 ms, and it will diffuse with a distance of $\sqrt{Z}\,\bar{\lambda} = 4$ mm. The diffusing distance is much less than the size of the photolytic zone and the IR collecting area. So the diffusion effect was omitted.

The quenching effect by other photolytic products was also neglible because about 1% of the precursor gas $CHBr_3$ was photolyzed, while the precursor gas only had a small ratio of 2.5% in the mixed gases.

In the CO_2 quenching experiment, about 7.7% of O_2 was added for producing CO(v). For low vibrational levels $v \leq 4$, the contribution of oxygen to the CO(v) relaxation was less than 5%. For the high vibrational levels, a modification considering the O_2 contribution to the rate constants has already been made.

Unlike Murphy's integral method,[10] here we suggest a differential method to solve the rate equations. The solving procedures are the following: (a) Arbitrarily give a set of quenching rate constants and a set of initial populations for each vibrational level. The A_v values are adapted from the ref 9. (b) Solving the rate equations 1−4 by the fourth-order Rung−Kutta method[33] to get the temporal vibrational populations. (c) Optimize the least-squares $F(v,t) = \sum_v [n_v^{\mathrm{cal}}(t) - n_v^{\mathrm{exp}}(t)]^2/v$, where $n_v^{\mathrm{exp}}(t)$ is the vibrational population, obtained by the simulation of experimental spectrum, for the vth level at a specific time. Then a set of new rate constants and that of new populations are produced. The Powell method[33] was used in our calculation in order to improve the computing rate. (d) Repeat the steps b and c iteratively until the result converges.

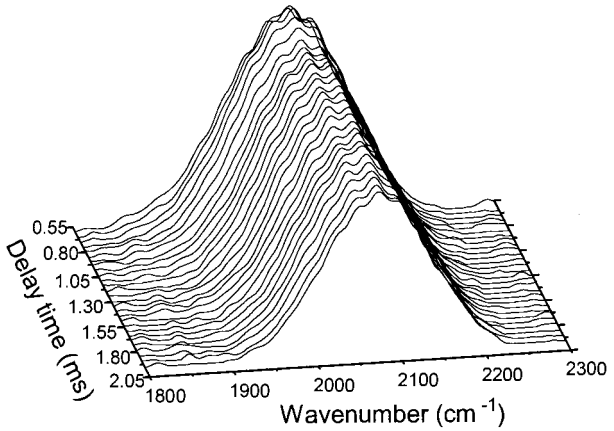

Figure 1. A set of time-resolved infrared emission spectra of CO($v \rightarrow v{-}1$). The delay time after the laser firing is indicated. The CO emission was quenched by excess oxygen gas. A gas mixture of 5 Pa $CHBr_3$/200 Pa O_2 was used.

The above differential method gives a better result than the integral method. No approximation is required for this differential method, while several rough approximations are made in Murphy's integral method, such as selecting a special integral time range. The results from the differential method are optimized by iteration so that they are more accurate than those from the integral method.

Equation 5 represents a set of linear equations. For a given set of n_v, the solution of the equations, i.e., k_v, is unique. An uncertainty of 10%−30% for the k_vs is estimated.

IV. Results and Discussion

1. The Generation of High Vibrationally Excited CO(v) Molecules. The vibrationally excited CO(v) were generated by 193 nm photoinduce chemical reaction of the mixtures of $CHBr_3$ and O_2.[34a,34b] Lin reported VUV photochemical reaction of $CHBr_3 + O_2$.[34a] They observed IR emission from the final product CO($v \leq 14$). However, to our knowledge, the reaction process is still of unknown. In the present experiment, the intense emission in the 1900−2200 cm^{-1} region from the vibrationally excited CO was observed. A spectral simulation indicated that the vibrational excitation of CO reached up to $v = 10$.

2. The Quenching of CO(v) by O_2. The quenching of the vibrationally excited CO(v) was investigated in the presence of excess oxygen. The vibrational relaxation can be studied through the decay of CO($v \rightarrow v{-}1$) emission. Figure 1 shows a set of time-resolved infrared spectra. Starting from 0.56 ms after the firing of the laser pulse, 28 sequential spectra were recorded with the time intervals of 0.05 ms. The emission intensity attained a maximum at 0.5 ms. After 0.6 ms, the decay of the emission is mainly ruled by the vibrational quenching.

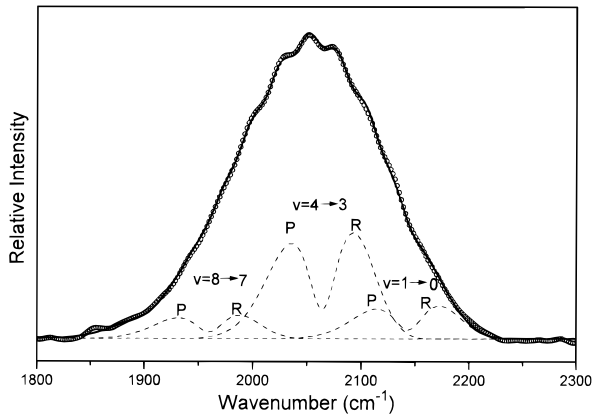

Figure 2. The experimental (circles) and the simulated (solid line) spectrum of the CO($v\rightarrow v-1$) emission for CO/O_2 system at a delay time of 0.86 ms. The contributions of some transitions to the simulated spectrum are shown by the dashed lines.

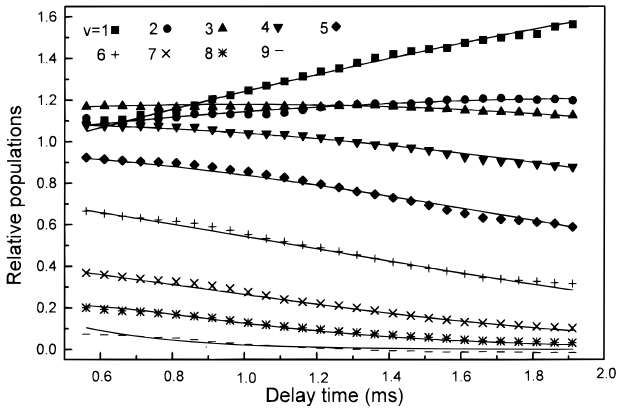

Figure 3. The vibrational population of CO(v) at different times for CO/O_2 system. The dots represent the experimental data obtained by the spectral simulation. The solid lines are obtained from the solution of the relaxation equations.

At each delay time, the relative population of each vibrational level of CO can be determined by spectral simulation.[29] In the simulation, the envelope of the emission is composed by the P and R branches of the individual rovibrational bands. We assumed that the rotation was completely relaxed to the room temperature of 300 K. A typical fitting spectrum is shown in Figure 2. A standard derivation of 5%−10% was given for the population.

Having simulated 28 spectra at different delay times, the evolution of the relative populations of CO(v=1−9) from 0.56 to 1.91 ms are obtained and shown in Figure 3. It is seen in the figure that the populations of the high vibrational levels $v = 4-10$ monotonically decay with time. For the level $v = 3$, the population increases in the first several hundred microseconds after we begin measuring and then decreases. The populations of the vibrational levels $v = 1$ and 2 increase constantly in the time range. The trend reflects that the vibrational relaxation of the higher levels are faster than those of the lower ones.

With the above population data, the rate eq 5 was solved by the differential method suggested in the section III. As a result, nine rate constants for CO(v) quenched by O_2 and a set of best-fitting vibrational populations were obtained and shown as the curves in the Figure 3. The quite good agreement with the data is obvious. This comparison not only demonstrates the quality of the rate fit to the data but also shows that the data can be adequately interpreted in terms of eq 5. If the relaxation mechanism were different than that assumed, the rates determined from the differential method would not properly reproduce the population time histories. The obtained quenching rate constants and the reported values by other authors are listed in Table 1.

TABLE 1: Quenching Rate Constants of CO(v) by O_2 in Units of cm^3 Molecule^{-1} s^{-1}

k_v	Bauer[5] ($\times10^{-15}$)	Donovan[6] ($\times10^{-14}$)	Miller[7] ($\times10^{-17}$)	Hancock[8] ($\times10^{-16}$)	Smith[9] ($\times10^{-14}$)	this work ($\times10^{-14}$)
k_1	1.5[a]	1.0[a]	7.8[a]	1.5[a]		1.1 ± 0.1
k_2						1.9 ± 0.1
k_3						2.0 ± 0.3
k_4						2.3 ± 0.3
k_5						2.5 ± 0.3
k_6						3.0 ± 0.3
k_7						4.0 ± 0.5
k_8						4.8 ± 0.5
k_9						8.0 ± 0.8
k_{12}					2.1	
k_{13}					4.4	

[a] The data are calculated by the formula $k_v = \sigma_v P_v$, $\sigma_v = 3.3 \times 10^{-10}$ cm^3 molecule^{-1} s^{-1}; P_vs are taken from the references indicated.

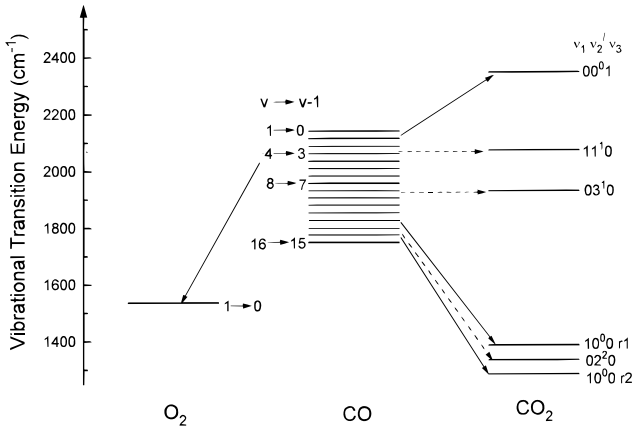

Figure 4. The energy diagram of the transitions between the vibrational excited CO(v) and the O_2, CO_2 molecules. The solid arrows show the preferential energy transfer channels. The dashed arrows indicate the multiquanta transitions.

The trend of the measured k_v values with v can be interpreted by energy defect theory. The energy defect ΔE in the exchange reaction of CO($v\rightarrow v-1$,v=1−10) and O_2($v = 1\leftarrow0$) is between 587 and 350 cm^{-1}, as shown in Figure 4. Usually, such moderate values corresponds to a medium V−V energy transfer rate constant. Furthermore, as the vibrational quantum number of CO(v) increases, the vibrational anharmonicity causes a reduction of ΔE, resulting in an increasing of the rate constants.

3. The quenching of CO(v) by CO_2. Now, excess CO_2 gas was introduced to the gas mixture to quench the vibrationally excited CO(v). Twenty-four spectra were recorded by TR FTIR spectrometer from a delay time of 0.1−4.7 ms with the time intervals of 0.2 ms. A typical spectrum is shown in Figure 5. The emission in the ranges 1900−2200 cm^{-1} and 2200−2500 cm^{-1} is assigned to the CO($v\rightarrow v-1$) and CO_2(ν_3,$v\rightarrow v-1$) transition, respectively. The excitation of CO_2(ν_3) is due to the collision energy transfer from CO(v).

The vibrational population of CO(v) is determined by spectral simulation. One of the simulated spectra is indicated in Figure 6. Figure 7 shows the temporal evolution of the vibrational populations. The populations almost decay monotonically.

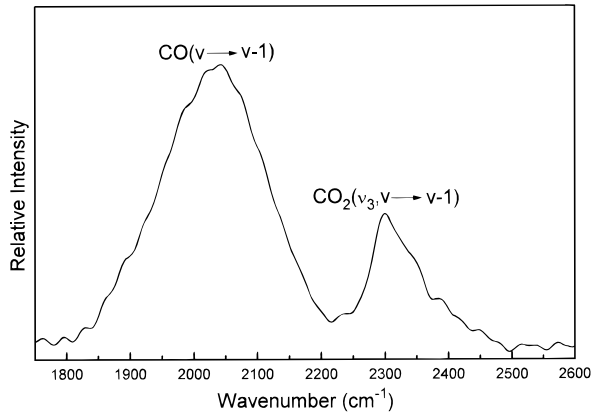

Figure 5. An infrared spectrum of the CO($v\rightarrow v-1$) emission (1900−2200 cm^{-1}) The vibrational energy was transferred to the ν_3 mode of CO_2(2250−2450 cm^{-1}). The spectrum was obtained from 193 nm photolysis of the mixture of 5 Pa $CHBr_3$, 20 Pa O_2, and 70 Pa CO_2 at a delay time of 0.1 ms.

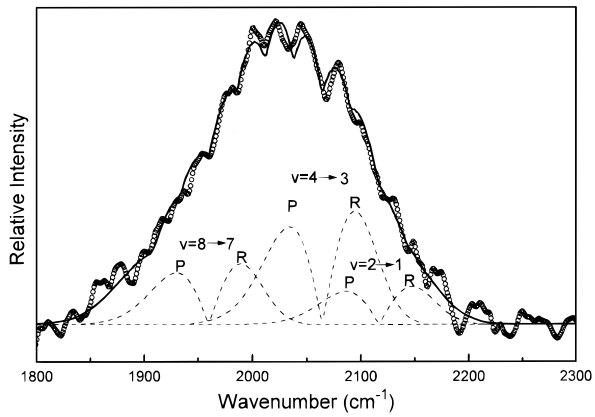

Figure 6. The experimental (circles) and the simulated (solid line) spectrum of the CO ($v\rightarrow v-1$) emission for CO/CO_2 system at 0.5 ms. The contributions of some transitions to the simulated spectrum are shown by the dashed lines.

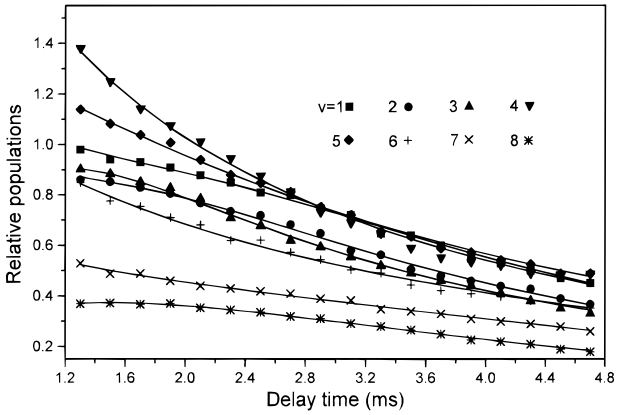

Figure 7. The vibrational population of CO(v) at different times for CO/CO_2 system. The dots represent the experimental data obtained by the spectral simulation. The solid lines are obtained from the solution of the relaxation equations.

The relaxation rate equations were solved again by the differential method in section III. Eight quenching rate constants were obtained.

The relation of log(k_v/v) to v is presented in Figure 8. Murphy and Smith's results are also shown in the figure. The vibrational relaxation rate of the middle levels(v = 5−8) of CO(v) is relatively low, while those of the low (v = 1−4) and high (v > 8) levels are high. The phenomenon indicates that

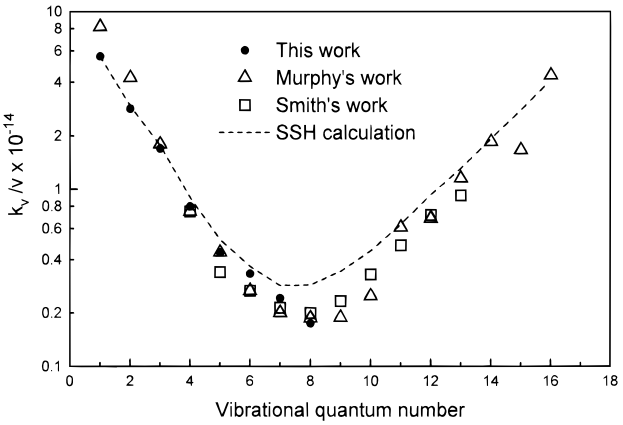

Figure 8. The logarithm of the reduced quenching rate constants k_v/v versus the vibrational quantum number v for the CO(v)/CO_2 system. The SSH theoretical data are linked by a dashed line.

there exist at least two competitive relaxation channels. For the low vibrational levels, the energy defect ΔE between CO($v\rightarrow v-1$) and CO_2(00°1←00°0) is relatively small (Figure 4). The vibrational energy prefers to transfer to the CO_2(ν_3) mode which has been observed in the spectrum (Figure 5). For the higher levels of CO(v), the energy defect become large, causing an unusual decreasing of the k_v/v with v. On the other hand, the defect in the energy exchange of CO($v\rightarrow v-1$) and CO_2-(10°0←00°0) is getting smaller (Figure 4). Therefore, for these highly vibrationally excited CO(v) molecules, the energy preferentially transfers to the ν_1 mode of CO_2. Due to symmetry, the 10°0 state mixes with the 02°0 state, forming two Fermi mixed states: 10°0 r1 (1388.3 cm^{-1}) and 10°0 r2 (1285.5 cm^{-1}).[35] Unfortunately the frequencies of these modes are too low so that we could not record them with our InSb detector.

The energy exchange processes with multiquanta transitions are also considered. Between the 10°0 r1 and the 10°0 r2 states, there exists another state 02^20 (1335.6 cm^{-1}), which may be reached via a two-quanta transition in the energy exchange process. For the middle CO(v) levels, two multiquanta channels of the energy transfer to the 11^10 (2076.5 cm^{-1}) and 03^10 (1932.5 cm^{-1}) probably occur due to accidental resonance. However, the low relaxation rate constants for these levels imply that the multiquanta transitions are not efficient.

On the basis of the above multilevel relaxation model, a modified Schwartz−Slawsky−Herzfeld (SSH) calculation[36−38] was performed. In the calculation, a Morse intermolecular potential and the vibrational anharmonicity were considered. The resulting probability of the V−V relaxation is given by

$$P(v_m) = 4\pi^2 a^4 S_A S_B F(v_m, v, D_e, r_e, a) \quad (6)$$

where F is a function of D_e, the Morse potential well depth; r_e, the equilibrium distance; a, the range parameter; v_m, initial relative velocity; and v, the vibrational level of CO molecular. S_A and S_B are the steric factors of the collision partners A and B, representing the average rotational contribution.

After averaging the overall initial velocities at temperature T, the result is

$$\langle P(T)\rangle = (\mu_v/2kT)^2 \int v_m 3\, P(v_m) \exp(-\mu_v v_m{}^2/2kT)\, dv_m \quad (7)$$

Then the V−V rate constant is obtained by

$$k(T) = \langle P(T)\rangle (8\pi kT/\mu_v)^{1/2} \sigma_{AB}{}^2 \quad (8)$$

TABLE 2: Parameters Used in the SSH Theoretical Calculation for the CO(v)/CO_2 System

molecule	mass (amu)	ν (cm^{-1})	A (amu^{-1})	S_A, S_B	LJ(12−6) potential[b] ϵ(cal mol^{-1})	σ(nm)
CO	28	2143	0.074	$^1/_3$	175	0.3706
		ν_1 1388	0.031[a]	$^1/_3$		
CO_2	44	ν_2 667	0.009[a]	$^2/_3$	378	0.3996
		ν_3 2349	0.009[a]	$^1/_3$		

Morse potential range parameter $\alpha = 22\ nm^{-1}$

[a] Reference 40. [b] Reference 41.

With the parameters in Table 2, the calculations have been carried out on the two major paths, CO(v)→CO_2(00°1) and CO(v)→CO_2(10°0 r1). The contribution of CO(v)→CO_2-($11^10,03^10$) was estimated by a general SSH theory.[39] The CO(v)→CO2(10°0 r2, 02^20) channels were not considered. The theoretical results of the relaxation rate constants of CO(v) are shown in Figure 8. It is seen that the calculated data are in good agreement with experimental results. The mechanism of the vibrational quenching of CO(v) by CO_2 can be reasonably explained by a multichannel model of energy exchange.

V. Conclusion

Time-resolved Fourier transform infrared emission spectroscopy has been applied to study the relaxation of the highly vibrationally excited carbon monoxide. The spectra were simulated to determine the vibrational populations. The rate equations were numerically solved by a new method, and the rate constants for the relaxation of CO(v) by O_2 for $v = 1-9$ and by CO_2 for $v = 1-8$ were determined.

A single-channel model of the energy transfer mechanism explained the trend of k_v s for the CO(v)/O_2 system. For the CO(v)/CO_2 system, there existed several competitive relaxation channels. For the low vibrational levels of CO, the energy of CO(v) transferred mainly to CO_2(00°0)→(00°1). For the high vibrational levels of CO, the energy transferred mainly to CO_2(00°0)→(10°0 r1) or its Fermi mixed partner (10°0 r2). Some multiquanta channels, transferring energy to CO_2-($02^20,11^10,03^10$), also had some contributions to the energy exchange process.

Acknowledgment. The paper was carefully reviewed by Prof. Qihe Zhu, and the experiment was helped by H.M. Su and Dr. Q. Li. We deeply appreciate their efforts. This work is supported by the National Natural Science Foundation of China.

References and Notes

(1) Taylor, R. L.; Bitterman, S. *Rev. Mod. Phys.* **1969**, *41*, 26.
(2) Ormonde, S. *Rev. Mod. Phys.* **1975**, *47*, 193.
(3) Taylor, R. L. *Can. J. Chem.* **1974**, *52*, 1436.
(4) Flynn, G. W.; Parmenter, C. S.; Wodtke, A. M. *J. Phys. Chem.* **1996**, *100*, 12817.
(5) Bauer, H. J.; Roesler, H. *Molecular Relaxation Processes*; Academic Press: New York, 1966.
(6) Donovan, R. J.; Husain, D. *Trans. Faraday Soc.* **1967**, *63*, 2879.
(7) Miller, D. J.; Millikan, R. C. *Chem. Phys. Lett.* **1974**, *27*, 10.
(8) Green, W. H.; Hancock, J. K. *J. Chem. Phys.* **1973**, *59*, 4326.
(9) Hancock, G.; Smith, I. W. M. *Appl. Opt.* **1971**, *10*, 1827.
(10) Caledonia, G. E.; Green, B. D.; Murphy, R. E. *J. Chem. Phys.* **1979**, *71*, 4369.
(11) Nowlin, M. L.; Heaven, M. C. *J. Chem. Phys.* **1993**, *99*, 5654.
(12) Nowlin, M. L.; Heaven, M. C. *J. Phys. IV* **1994**, *4*, C4.
(13) Nowlin, M. L.; Heaven, M. C. *Chem. Phys. Lett.* **1995**, *239*, 1.
(14) Yang, X.; Wodtke, A. M. *Int. Rev. Phys. Chem.* **1993**, *12*, 123.
(15) Yang, X.; Price, J. M.; Mack, J. A.; Morgan, C. G.; Rogaski, C. A.; McGuire, D.; Kim, E. H.; Wodtke, A. M. *J. Phys. Chem.* **1993**, *97*, 3944.
(16) Yang, X.; Kim, E. H.; Wodtke, A. M. *J. Chem. Phys.* **1990**, *93*, 4483.
(17) Yang, X.; Wodtke, A. M. *J. Chem. Phys.* **1990**, *92*, 116.
(18) Yang, X.; Kim, E. H.; Wodtke, A. M. *J. Chem. Phys.* **1992**, *96*, 5111.
(19) Yang, X.; Rogaski, C. A.; Wodtke, A. M. *J. Opt. Soc. Am. B* **1990**, *7*, 1835.
(20) Hartland, G. V.; Dong, Q.; Dai, H. L. *J. Chem. Phys.* **1995**, *102*, 8677.
(21) Hartland, G. V.; Dong, Q.; Dai, H. L. *J. Chem. Phys.* **1994**, *101*, 8554.
(22) Hartland, G. V.; Qin, D.; Dai, H. L. *J. Chem. Phys.* **1994**, *100*, 7832.
(23) Rogaski, C. A.; Price, J. M.; Mack, J. A.; Wodtke, A. M. *Geophys. Res. Lett.* **1993**, *20*, 2885.
(24) Price, J. M.; Mack, J. A.; Rogaski, C. A.; Wodtke, A. M. *Chem. Phys.* **1993**, *175*, 83.
(25) Rogaski, C. A.; Mack, J. A.; Price, J. M.; Wodtke, A. M. *Faraday Discuss.* **1998**. In press.
(26) Park, H.; Slanger, T. G. *J. Chem. Phys.* **1994**, *100*, 287.
(27) Klatt, M.; Smith, I. W. M.; Symonds, A. C.; Tucket, R. P.; Ward, G. N. *J. Chem. Soc., Faraday Trans.* **1998**. In press.
(28) Klatt, M.; Smith, I. W. M.; Tucket, R. P.; Ward, G. N. *Chem. Phys. Lett.* **1994**, *224*, 253.
(29) Wang, X. B.; Li, H. Z.; Ju, Q.; Zhu, Q. H.; Kong, F. A. *Chem. Phys. Lett.* **1993**, *208*, 290.
(30) Leone, S. R. *Acc. Chem. Res.* **1989**, *22*, 139.
(31) Sloan, J. J. *J. Chem. Phys.* **1986**, *84*, 1412.
(32) Zhu, Q. H.; Huang, S. L.; Wang, X. B.; Hao, Z.; Zhang, Q. F.; Cao, J. R.; Wu, X. J.; Lu, N.; Yao, S. X.; Kong, F. A. *Chinese J. Chem. Phys.* **1993**, *6*, 87.
(33) Press: W. H.; Flannery, B. P.; Teukolsky, S. A.; Vetterling, W. T. *Numerical Recipes*; Cambridge University: New York, 1986.
(34) (a) Lin, M. C. *J. Chem. Phys.* **1974**, *61*, 1835. (b) Li, H. Z.; Wang, X. B.; Kong, F. A.; Zhu, Q. H. *Acta Phys.−Chim. Sin.* **1993**, *9*, 452.
(35) Herzberg, G. *Molecular Spectra and Molecular Structure, II: Infrared and Raman Spectra of Polyatomic Molecules*; D. Van Nostrand Company, Inc.: New York, 1966.
(36) Devonshire, A. F. *Proc. R. Soc. London, Ser. A* **1937**, *158*, 269.
(37) Thompson, S. L. *J. Chem. Phys.* **1968**, *49*, 3400.
(38) Abdel-Halim, H.; Ewing, G. E. *J. Chem. Phys.* **1985**, *82*, 5442.
(39) Schwartz, R. N.; Slawsky, Z. I.; Herzfeld, K. F. *J. Chem. Phys.* **1952**, *20*, 1591.
(40) Carlos, M.; Hernando, P.; Juan, F.; Carlos G.; Engenio, S. *J. Chem. Phys.* **1983**, *78*, 5971.
(41) Hirschfelder, J. O.; Lartiss, C. F.; Bird, R. B. *Molecular Theory of Gases and Liquids*; Wiley: New York, 1954.